Supplementary Information

Imaging Mass Spectrometry Reveals Complex Lipid Distributions Across *Staphylococcus aureus* Biofilm Layers

Emilio S. Rivera[1,2], Andy Weiss[3], Lukasz G. Migas[4], Jeffrey A. Freiberg[3], Katerina V. Djambazova[2,5], Elizabeth K. Neumann[1,2], Raf Van de Plas[2,4], Jeffrey M. Spraggins[1,2,5,8*], Eric P. Skaar[3], and Richard M. Caprioli[1,2,5,6,7]

[1]Department of Biochemistry, Vanderbilt University, [2]Mass Spectrometry Research Center, Vanderbilt University, [3]Department of Pathology Microbiology and Immunology, Vanderbilt University, [4]Delft University of Technology, Delft, Netherlands, [5]Department of Chemistry, Vanderbilt University, [6]Department of Medicine, Vanderbilt University, [7]Department of Pharmacology, Vanderbilt University, [8]Department of Cell and Developmental Biology, Vanderbilt University

*Corresponding Author: Jeffrey M. Spraggins, jeff.spraggins@vanderbilt.edu

Figure S1. Comparison of CFU of aerobic and anaerobic biofilms, and photos of biofilms during development;

Figure S2. Autofluorescence microscopy for biofilm structure retention through sample preparation, ion image of spectral interference at *m/z* 325.07, and comparative spectra between DAN and DHA;

Figure S3. Comparison of signal intensity between washed and unwashed for *m/z* 1351.96;

Figure S4. MALDI spectra comparing convoluting peaks between DAN and DHA;

Figure S5. MALDI spectra comparing S/N and peak capacity with and without the TIMS dimension;

Figure S6. Replicates of ROIs and extracted ion mobilograms for each cardiolipin;

Table S1. List of putatively identified bacterial lipids with ppm error ;

Figure S7. MS/MS fragmentation spectra;

Figure S8. Fluorescence microscopy and MALDI TIMS IMS of a cross-section of a transgenic strain of USA300 LAC expressing GFP;

Figure S9. Ion images of cardiolipin distributions that do not localize according to odd/even-chain trend;
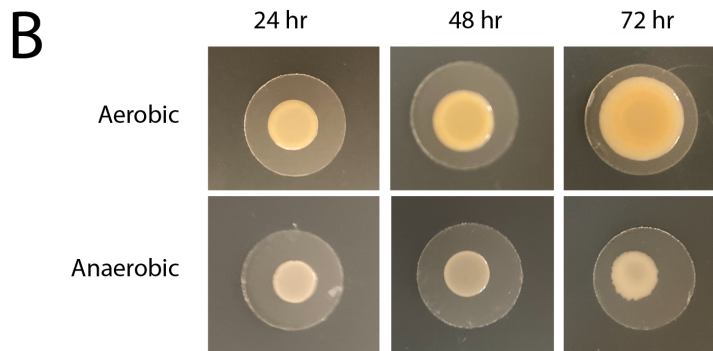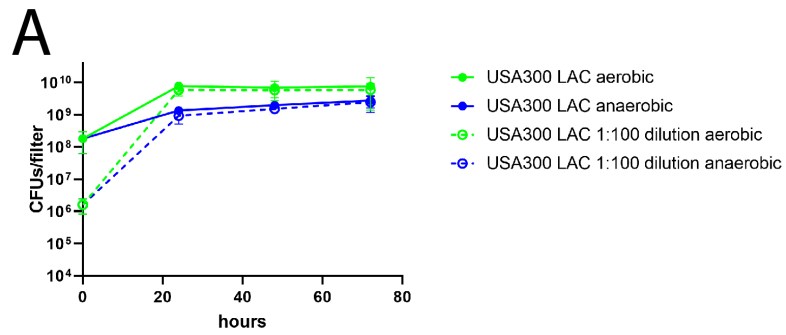
Figure S10. Replicate experiment of cardiolipin abundance comparisons between layers;

Figure S11. Mass spectra of each CL species measured in Figure 5;

Figure S12. IMS of biological replicates of *S. aureus* biofilms grown with USA300 LAC and USA300 JE2;

Figure S13. *k*-means clustering of anaerobic biofilm;

Figure S14. MALDI IMS burn patterns.

Figure S1. Comparison of CFUs per biofilm grown for 24, 48, and 72 hr under aerobic conditions (green) and anaerobic conditions (blue) (**A**). Experiment was performed in biological triplicate; missing error bars are due to error bars being smaller than the point on the graph. Pictures of *S. aureus* biofilms taken at each transfer time point during development (24 hr, 48 hr, and 72 hr) (**B**).
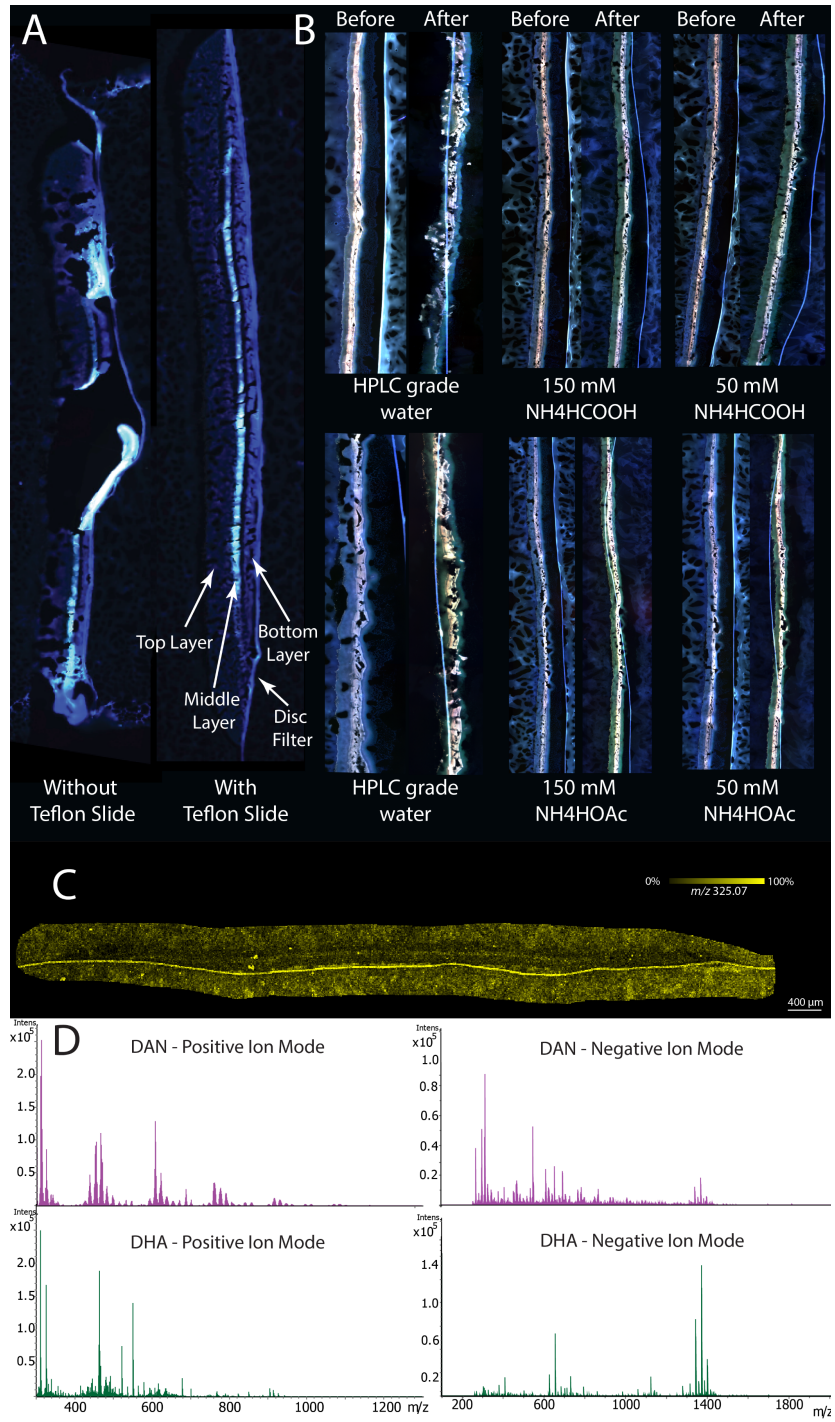
Figure S2. Autofluorescence of an *S. aureus* biofilm without, and with even adherence provided by the teflon-coated slide, showing reduced shriveling of the biofilm with the Teflon-coated slide (**A**); Autofluorescence before and after washing with HPLC grade water, 150 mM and 50 mM ammonium formate (NH₄HOOH) and ammonium acetate (NH₄OAc) (**B**); Ion image of *m/z* 325.07, showing localization to the filter disc and matrix around the biofilm (**C**); averaged mass spectra of positive and negative-ion mode MALDI analysis of *S. aureus* biofilms with DAN matrix (purple) and DHA matrix (green) demonstrating matrix clusters throughout the spectrum when DAN was used (**D**).
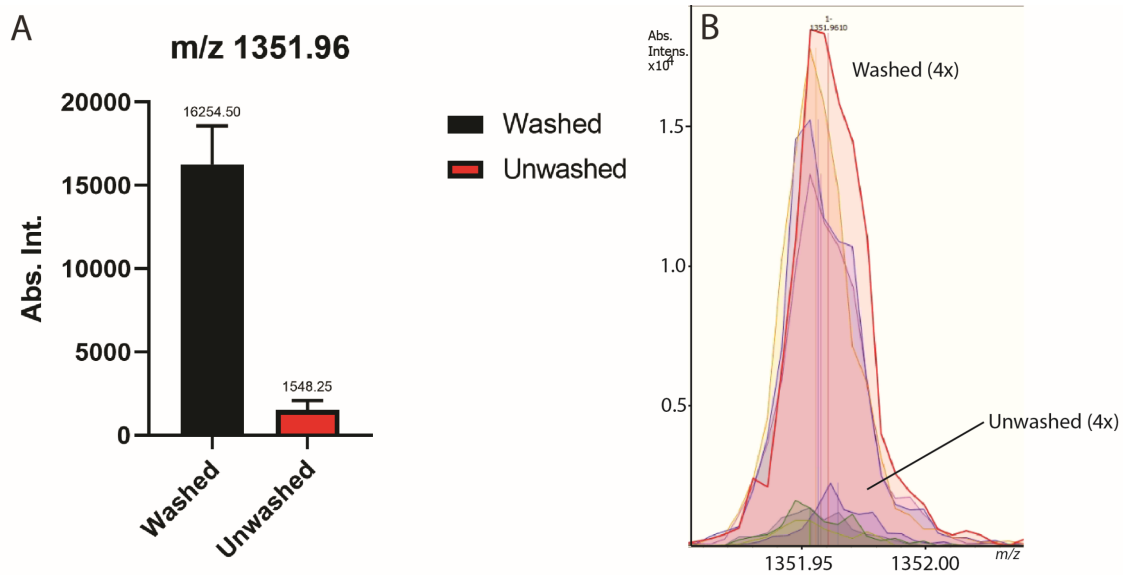
Figure S3. Comparison of signal intensity measured for CL(64:0) at *m/z* 1351.96 between washed and unwashed samples where four biofilm serial sections were analyzed for each group. A bar graph demonstrates a difference of over 10-fold between washed and unwashed sample means (p = 0.0006) (**A**) and the resulting spectra for each replicate zoomed in on *m/z* 1351.96, where each replicate peak can be seen.
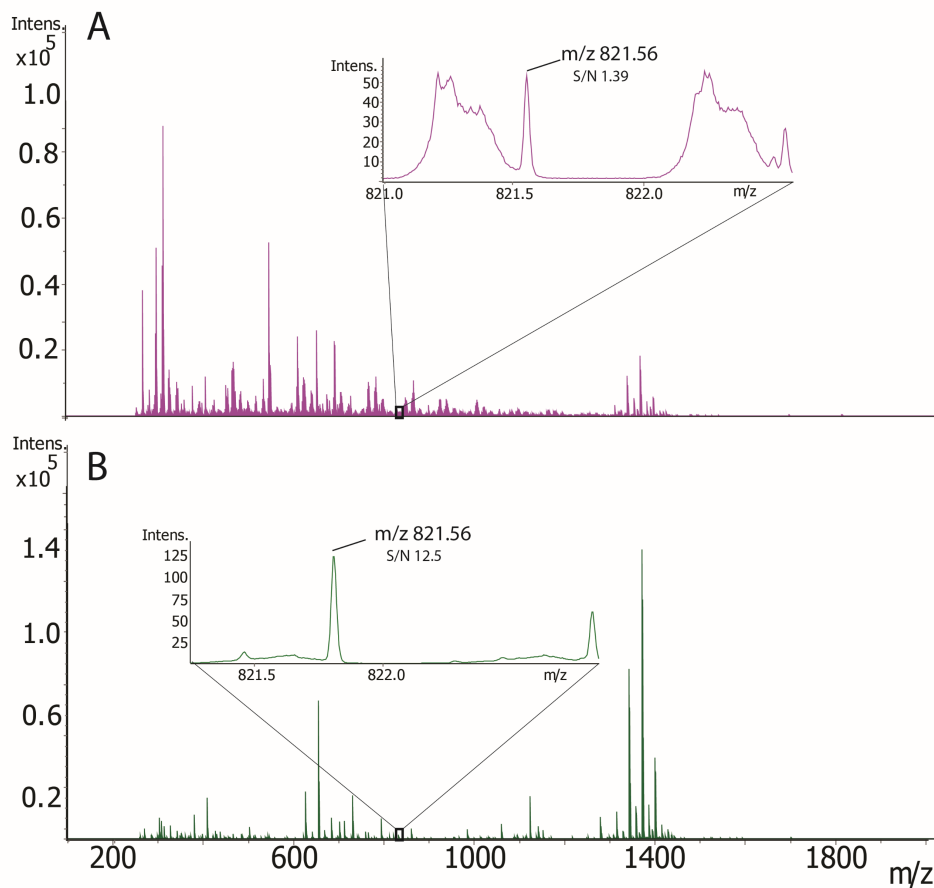
Figure S4. Averaged mass spectra of negative-ion mode MALDI analysis of *S. aureus* biofilms with DAN matrix (purple) and DHA matrix (green) with spectra zoomed in on Lysyl-PG(30:0) (*m/z* 821.56) demonstrates spectral interferences around the peak of interest and low S/N in the data acquired with DAN (**A**), and no such interfering peaks in the data acquired with DHA (**B**).
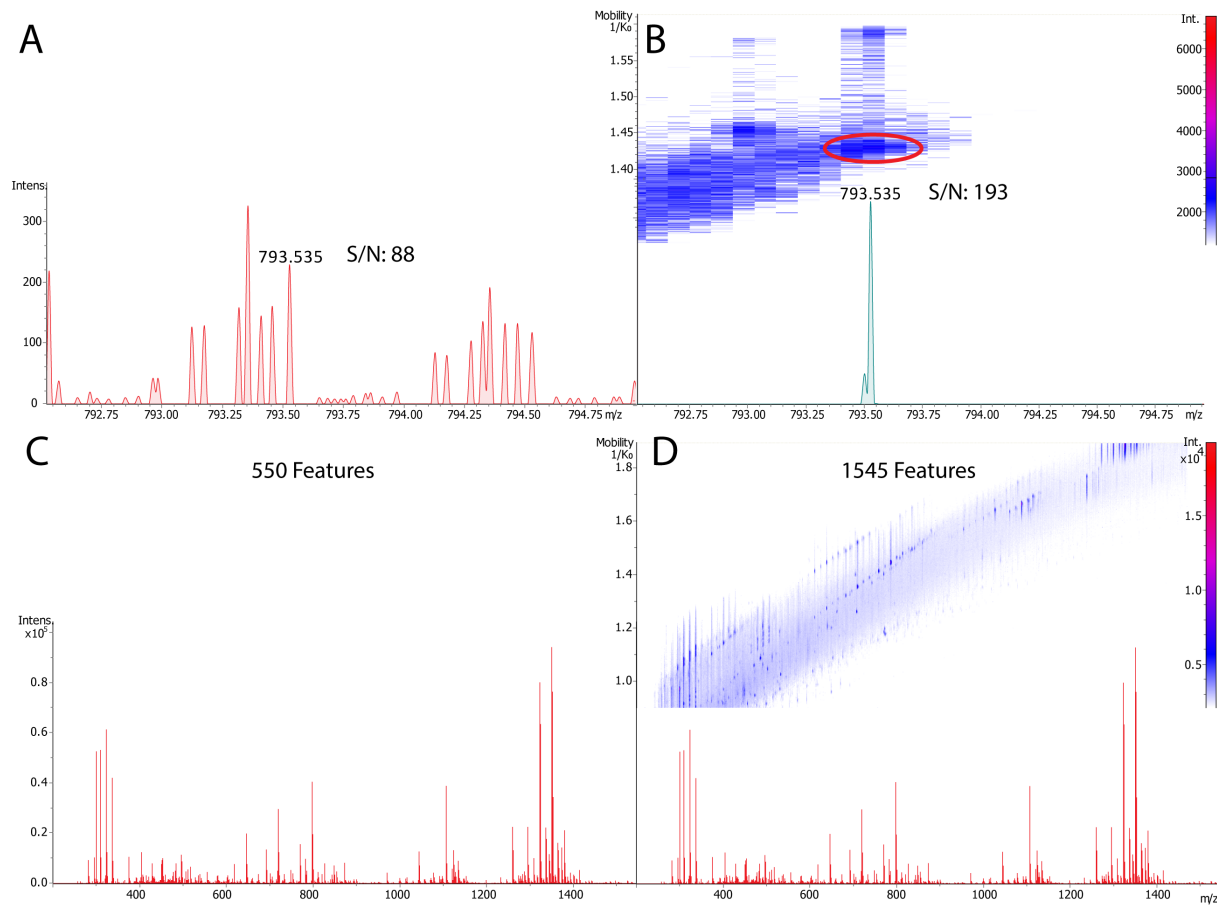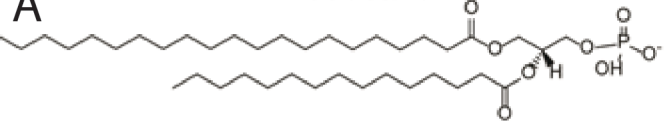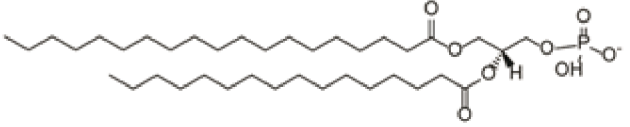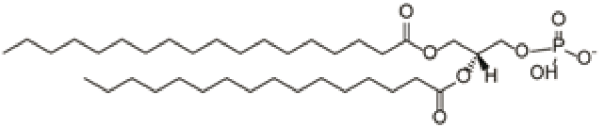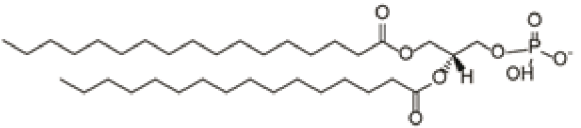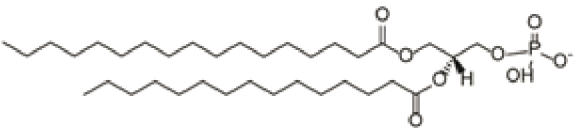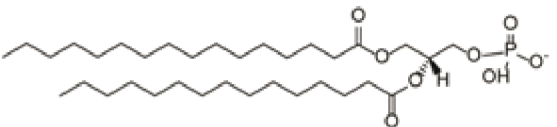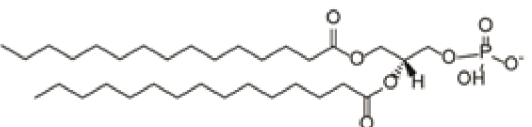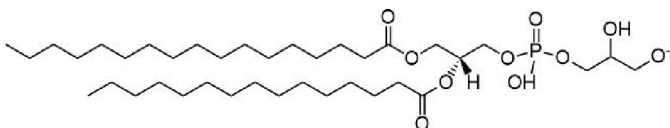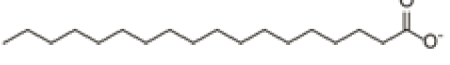
Figure S5. Averaged mass spectrum of a negative-ion mode IMS experiment of *S. aureus* biofilm, zoomed in to range *m/z* 792.5 – 795.0 showing L-PG(28:0) with a S/N of 88 without the TIMS dimension considered (**A**), and S/N of 193 when the TIMS dimension is considered (**B**). Averaged mass spectrum of the same negative-ion mode IMS experiment as above with 550 features detected when no TIMS was considered (**C**), and 1,545 features when TIMS was considered (**D**).
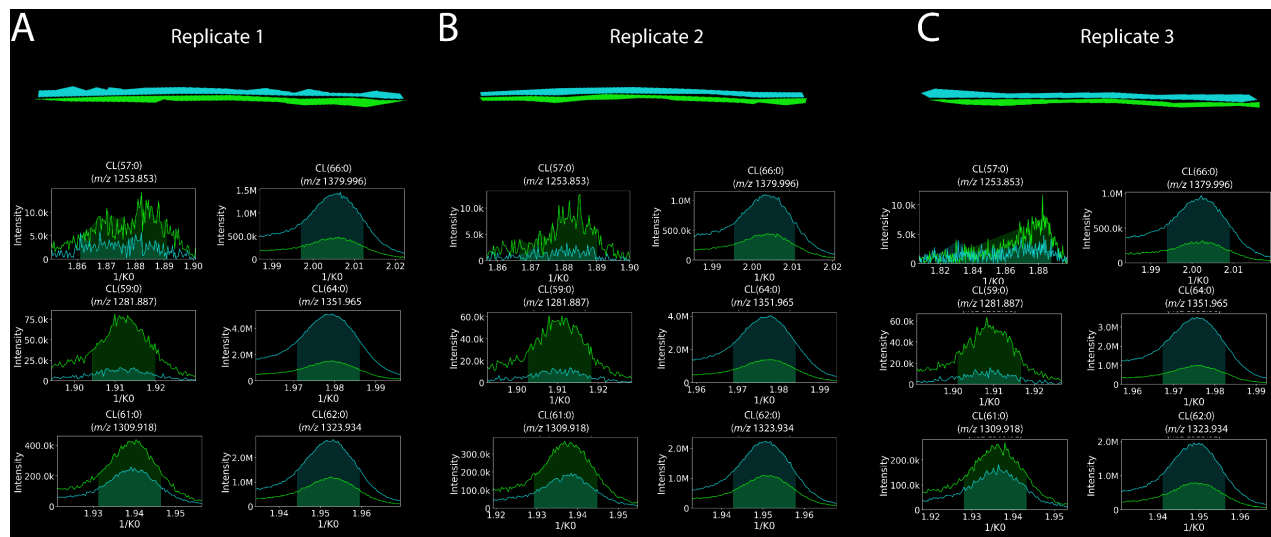
Figure S6. Regions of interest drawn for data extraction of top and bottom layers for lipidomic comparison and extracted ion mobilograms for each CL lipid of interest showing $1/K_0$ window selected for each ion from each o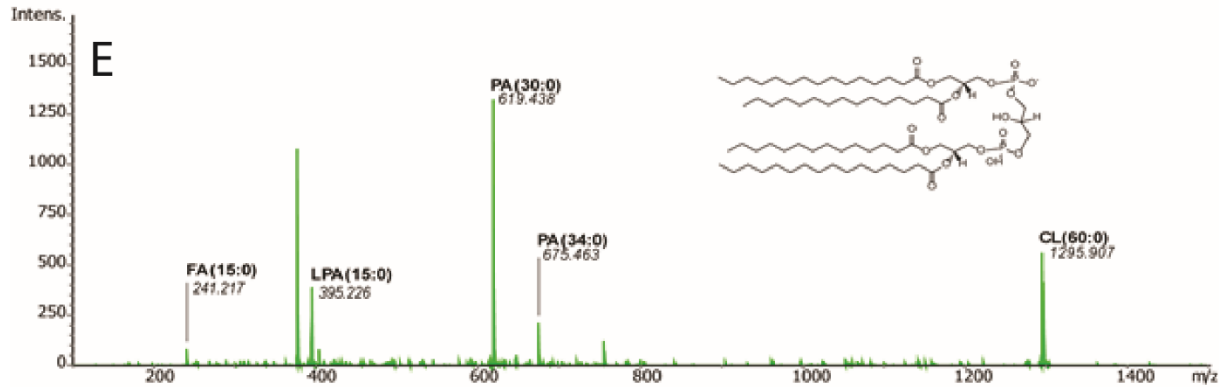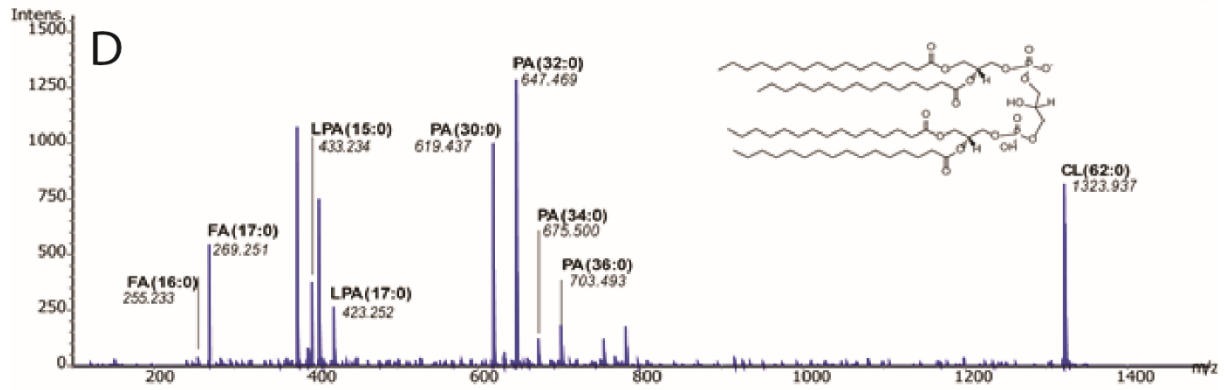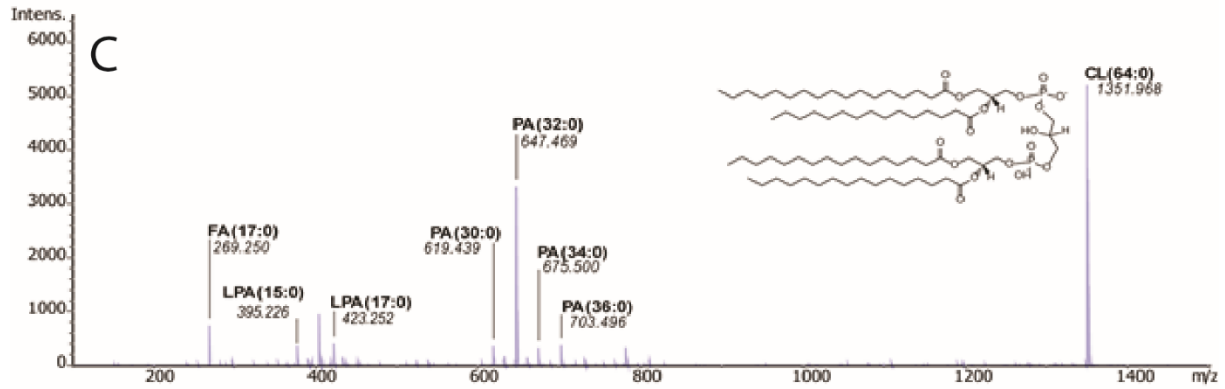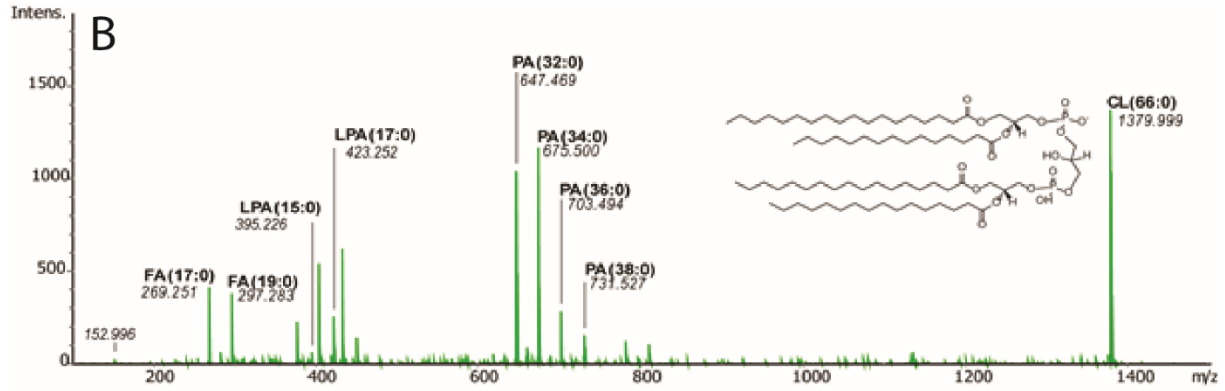f the three replicates performed (**A-C**). These data were used to generate violin plots in **Figure 5** and **Figure S10**.

ID	Observed *m/z*	Adduct	Theoretical *m/z*	ppm Error	$1/K_0$	MS/MS
DG(33:0)	565.52	[M+H-H_2O]^+	565.519	1.77	1.36	N
DGDG(32:0)	915.602	[M+Na]^+	915.6015	0.55	1.64	N
DG(32:0)	551.504	[M+H-H_2O]^+	551.5034	1.09	1.34	N
CL(60:0)	1295.903	[M-H]^-	1295.9024	0.46	1.86	Y
PIP(43:0)	1043.653	[M-H]^-	1043.657	3.83	1.68	N
PG(32:0)	721.5026	[M-H]^-	721.5025	0.14	1.35	Y
CL(57:0)	1253.853	[M-H]^-	1253.8554	1.91	1.88	N
CL(59:0)	1281.887	[M-H]^-	1281.8866	0.31	1.91	Y
CL(61:0)	1309.918	[M-H]^-	1309.9188	0.61	1.94	Y
CL(62:0)	1323.934	[M-H]^-	1323.9337	0.23	1.95	Y
CL(64:0)	1351.965	[M-H]^-	1351.965	0	1.98	Y
CL(66:0)	1379.996	[M-H]^-	1379.9963	0.22	2.01	Y

Table S1: Details pertaining to each lipid depicted in **Figures 3**, **4** and **6**.

A	Structure		Theoretical *m/z*
		PA(36:0)	703.5283
		PA(35:0)	689.5126
		PA(34:0)	675.4970
		PA(33:0)	661.4813
		PA(32:0)	647.4657
		PA(31:0)	633.4500
		PA(30:0)	619.4344
		PG(32:0)	721.5025
		FA(15:0)	241.2173
		FA(16:0)	255.2329
		FA(17:0)	269.2486
		FA(18:0)	283.2642

B

FA(17:0)
269.251

FA(19:0)
297.283

LPA(15:0)
395.226

LPA(17:0)
423.252

PA(32:0)
647.469

PA(34:0)
675.500

PA(36:0)
703.494

PA(38:0)
731.527

CL(66:0)
1379.999

152.996

C

FA(17:0)
269.250

LPA(15:0)
395.226

LPA(17:0)
423.252

PA(30:0)
619.439

PA(32:0)
647.469

PA(34:0)
675.500

PA(36:0)
703.496

CL(64:0)
1351.968

D

FA(16:0)
255.233

FA(17:0)
269.251

LPA(15:0)
433.234

LPA(17:0)
423.252

PA(30:0)
619.437

PA(32:0)
647.469

PA(34:0)
675.500

PA(36:0)
703.493

CL(62:0)
1323.937

E

FA(15:0)
241.217

LPA(15:0)
395.226

PA(30:0)
619.438

PA(34:0)
675.463

CL(60:0)
1295.907

Figure S7. Representative chemical structures of CL lipids (**A**) MS/MS for CL(66:0) (**B**), CL(64:0) (**C**), CL(62:0) (**D**), CL(60:0) (**E**), CL(61:0) (**F**), CL(59:0) (**G**) and PG(32:0) (**H**). Chemical structures shown above are not confirmed, but only representative structures based on *m/z*.
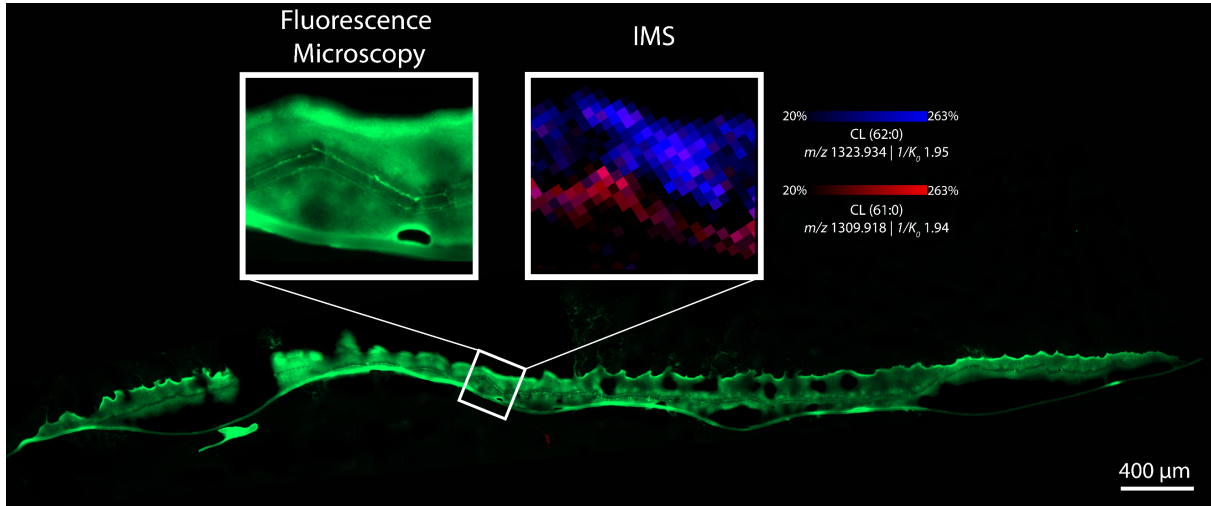
Figure S8. Fluorescence microscopy of an *S. aureus* biofilm grown with a strain of USA300 LAC that was genetically modified to constitutively express green fluorescent protein (GFP). Lower GFP signal in the middle layer of the biofilm suggests fewer bacteria in this region of the cross-section, and this corresponds with the absence of CL signal observed in the middle layer of the biofilms.
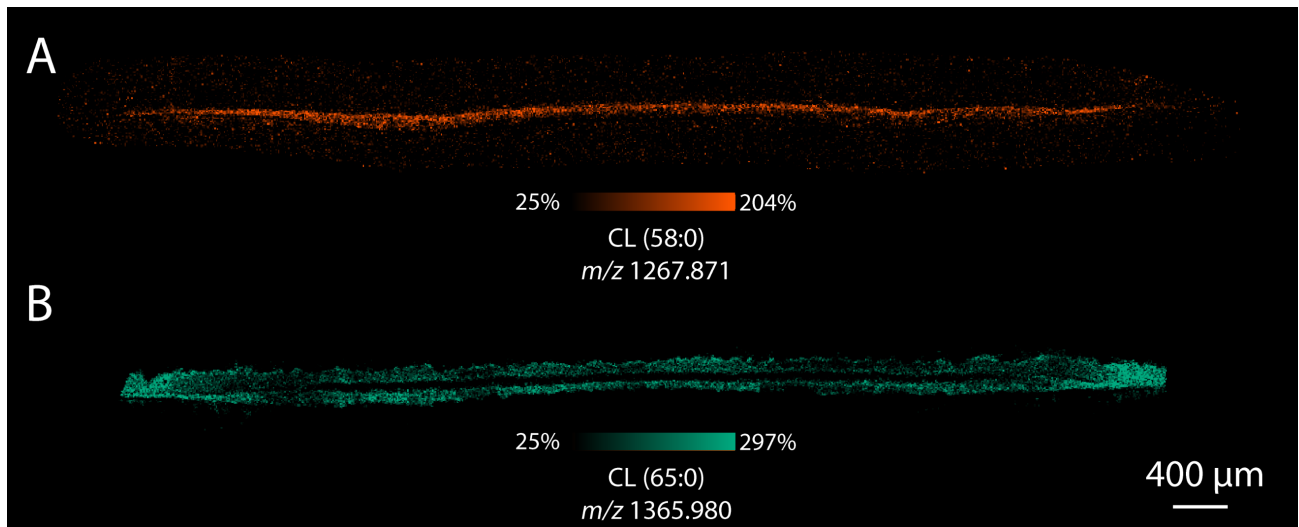

Figure S9. Ion image of CL(58:0) demonstrates that despite being an even-chain CL lipid it localizes primarily to the bottom layer of the biofilm (**A**), and CL(65:0) demonstrates that some cardiolipins have very similar abundance between top and bottom layers (**B**).
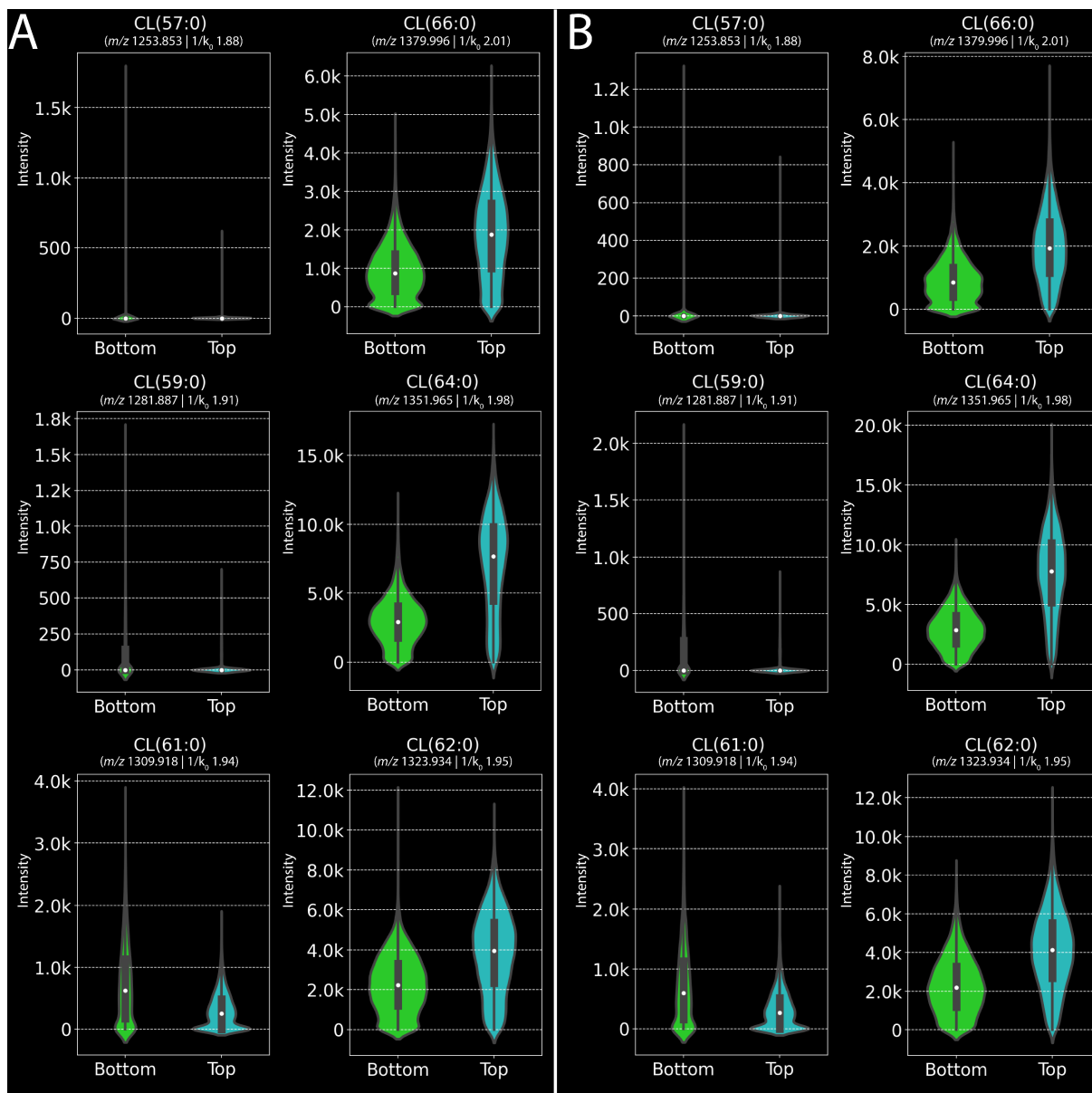
Figure S10. Violin plots generated from extracted data from Figure S4 for replicates 2 and 3.
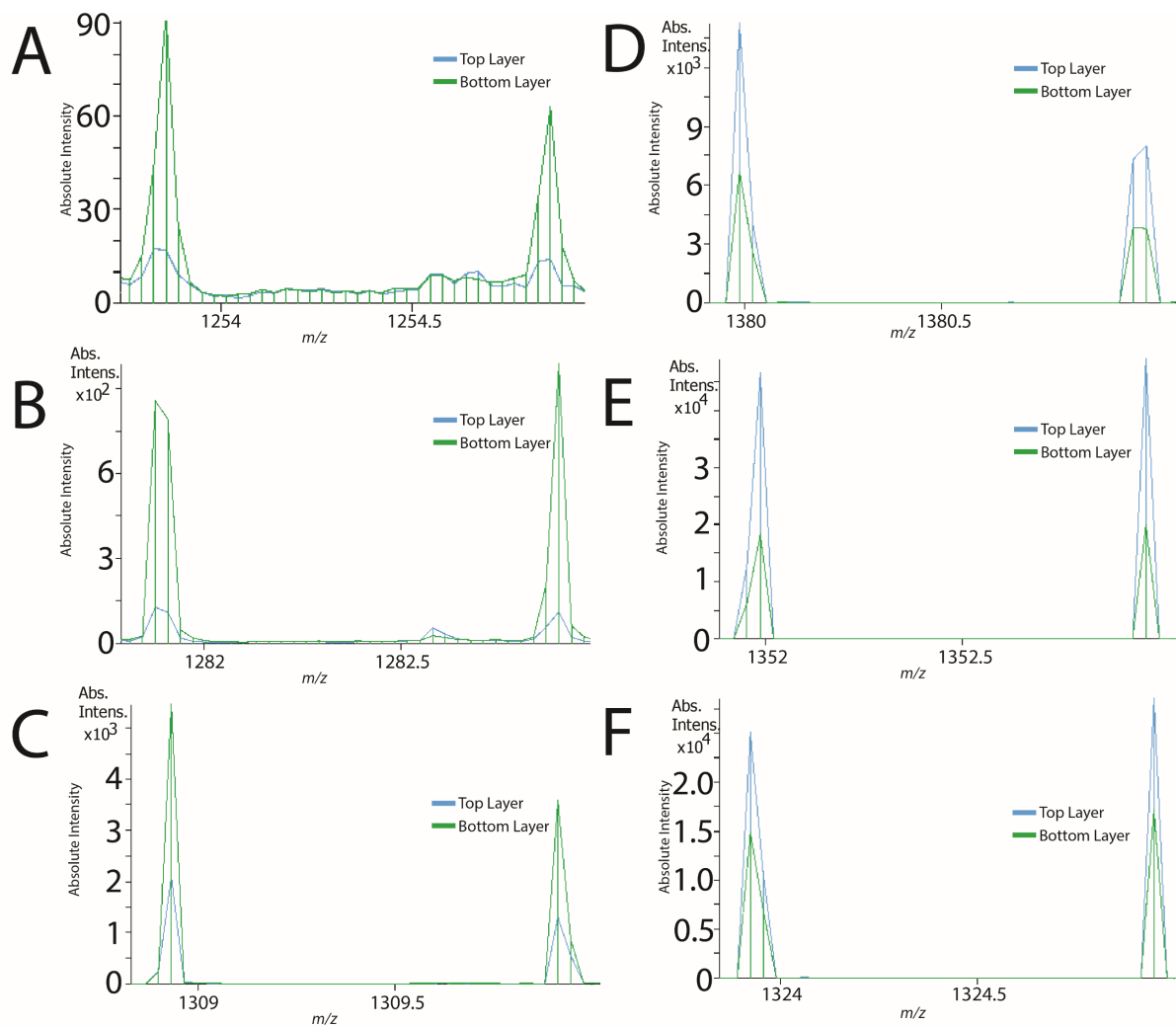
Figure S11. Zoomed in mass spectra on the monoisotopic peak and first isotopologue extracted from the top layer (green) and bottom layer (cyan) of each cardiolipin shown in Figure 5: CL(57:0), (**A**), CL(59:0) (**B**), CL(61:0) (**C**), CL(66:0) (**D**), CL(64:0) (**E**), and CL(62:0) (**F**).
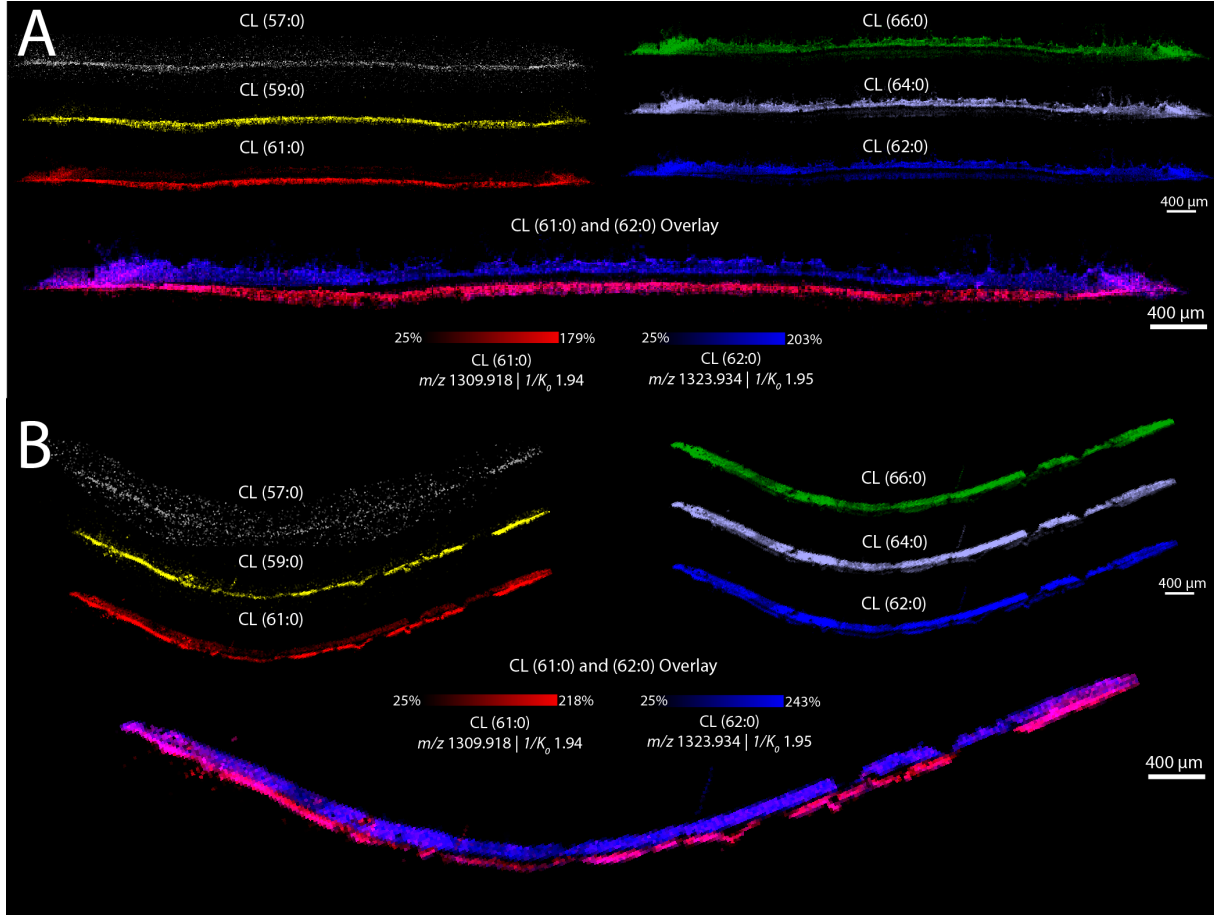
Figure S12. Biological replicates of *S. aureus* biofilms grown with USA300 LAC (A) and USA300 JE2 (B), demonstrating that the trends seen in cardiolipin distributions hold across not only a biological replicate, but a different strain of USA300 as well.
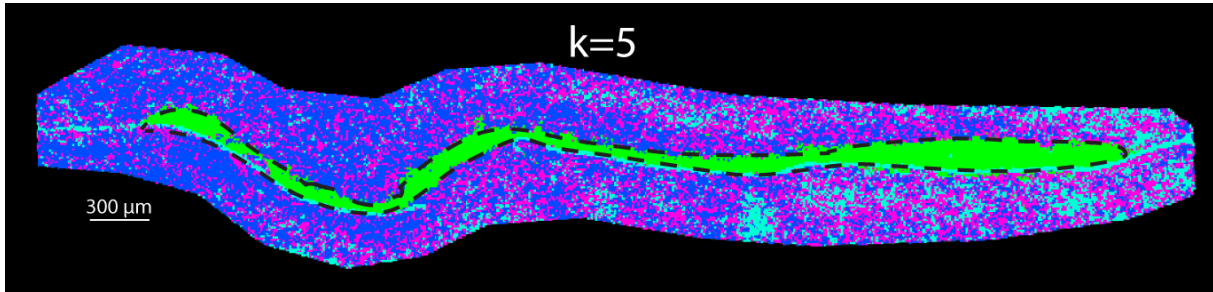
Figure S13. K-means clustering performed on IMS data of an anaerobic *S. aureus* biofilm as performed in Figure 2 (k=5) showing no segmentation of biofilm layers.
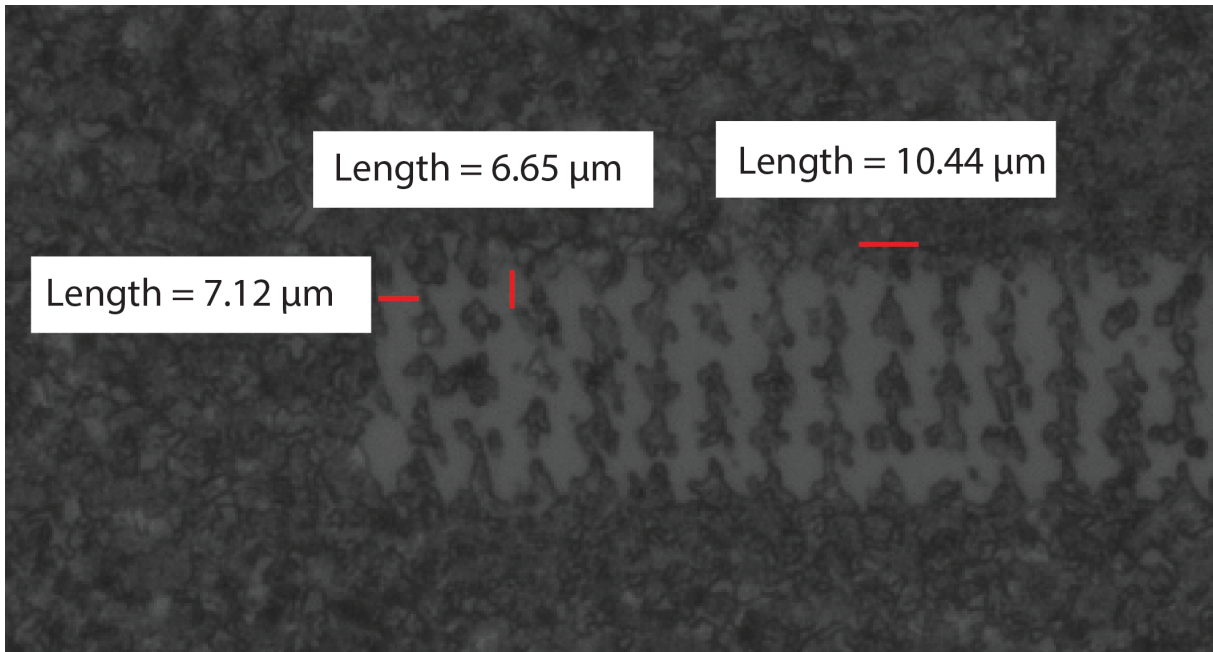
Figure S14. Burn patterns demonstrating a distance between pixels of ~10 µm and beam scan set to 6 x 6 µm resulting in an ablation area of approximately 7 x 7 µm.